



## Discovery of non-LBD inhibitor for androgen receptor by structure-guide design



Byung Jun Ryu<sup>c</sup>, Nakjeong Kim<sup>b</sup>, Jun Tae Kim<sup>a</sup>, Tae-Sung Koo<sup>a</sup>, Sung-Eun Yoo<sup>a</sup>, Seo Hee Jeong<sup>a</sup>, Seong Hwan Kim<sup>c</sup>, Nam Sook Kang<sup>a,\*</sup>

<sup>a</sup> Graduate School of New Drug Discovery and Development, Chungnam National Univ., Daehakno 99, Yuseong-gu, Daejeon 305-764, Republic of Korea

<sup>b</sup> Metabolic Syndrome Therapeutics Research Center, Bio-Organic Science Division, Korea Research Institute of Chemical Technology, P.O. Box 107, Yuseong-gu, Daejeon 305-600, Republic of Korea

<sup>c</sup> Laboratory of Translational Therapeutics, Pharmacology Research Center, Division of Drug Discovery Research, Korea Research Institute of Chemical Technology, P.O. Box 107, Yuseong-gu, Daejeon 305-600, Republic of Korea

### ARTICLE INFO

#### Article history:

Received 6 March 2013

Revised 11 April 2013

Accepted 25 April 2013

Available online 3 May 2013

#### Keywords:

Androgen receptor

BF-3 binding

LNCap cell

### ABSTRACT

In this study, we synthesized the BF-3 binding small molecules, a series of pyridazinone-based compounds, as a novel class of non-LBP antiandrogens for treating prostate cancer by inhibiting androgen receptor. The new class compound was discovered to inhibit the viability of AR-dependent human prostate LNCap cells and AR activity combining with the computational method. It showed a good physicochemical and PK property.

© 2013 Elsevier Ltd. All rights reserved.

Androgen receptor (AR) that belongs to the nuclear receptor superfamily of transcription factors is a major target for prostate cancer.<sup>1,2</sup> Prostate cancer (PCa) is the most popular cancer in men and one of the major causes of cancer related death.<sup>3</sup> AR structure consists of a variable amino-terminal activation function domain (AF-1), a highly conserved DNA-binding domain (DBD), a hinge region including the nuclear localization signal, a C-terminal ligand-binding domain (LBD) consisting of a 12 helical structure that surrounds a ligand binding pocket (LBP), a second activation function domain (AF-2) located at the carboxy terminal end of the LBD,<sup>4</sup> and a recently reported additional secondary binding function domain (BF-3) located on the surface of the AR controlling the allosteric modulation of the AF-2.<sup>5</sup> Until now, all clinically approved AR-targeting inhibitors directly block the binding of androgen to the ligand binding site of the receptor.<sup>6</sup> But the targeting the ligand binding pocket (LBP) has occurred several limitations such as drug resistance.<sup>7</sup> This is common problem for hormone nuclear receptor antagonists including AR and estrogen receptor antagonists. To overcome these limitations, AF-2 or BF-3 blocking small molecules without affecting natural ligand binding has been recently demonstrated as a novel class of non-LBP antiandrogens.<sup>8</sup>

Here, we discovered the BF-3 binding small molecules, a series of pyridazinone-based compounds, to inhibit the viability of LNCap

cells and AR activity combining with the computational method. Since LNCap cells are the representative AR-positive human prostate cancer cells lines, LNCap cells were used in this study. At early stage, we screened in-house compounds in LNCap cell. The most potent compound among the screened compounds was *N*-(3-(1-(4-cyanophenyl)-1-methyl-6-oxo-1,6-dihydropyridazin-4-yl)phenyl)ethanesulfonamide (**1**) as shown in Figure 1.

In the viability of LNCap cells, compound **1** exhibited the IC<sub>50</sub> value 39 μM when bicalutamide as a reference compound showed the IC<sub>50</sub> value 23 μM.<sup>9</sup> Next, to improve the inhibitory activity of compound **1** and its derivatives in LNCap cells, the docking experiment to evaluate its binding mode was carried out. First, we tried to dock at the LBP substituting androgen dihydrotestosterone (DHT) using the known X-ray crystallography structure, but the compound **1** was not fitted at the LBP of AR. We further explored the known surface binding site, AF-2 and BF-3, of AR and then found that the compound **1** can be well docked into BF-3 hydrophobic pocket of AR. Docking study was carried out from the X-ray crystal structure having a testosterone and a BF-3 binding small molecule (pdb code: 2YLQ).<sup>8</sup> The CDocker module<sup>10</sup> in Discovery Studio 3.5 with CHARMM force field was used. The ethane sulfonamide group of hit compound **1** interacts with side chain of N727 through hydrogen bonding and thus is expected to be good for binding with AR, as shown in Figure 2a. But, 4-cyanide group of phenyl ring of hit compound **1** is positioned nearby hydrophobic pocket. The phenyl ring bonded 4-cyanide group formed

\* Corresponding author. Tel.: +82 01072925756.

E-mail address: [nskang@cnu.ac.kr](mailto:nskang@cnu.ac.kr) (N.S. Kang).

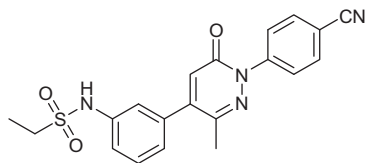


Figure 1. Primary hit compound (1).

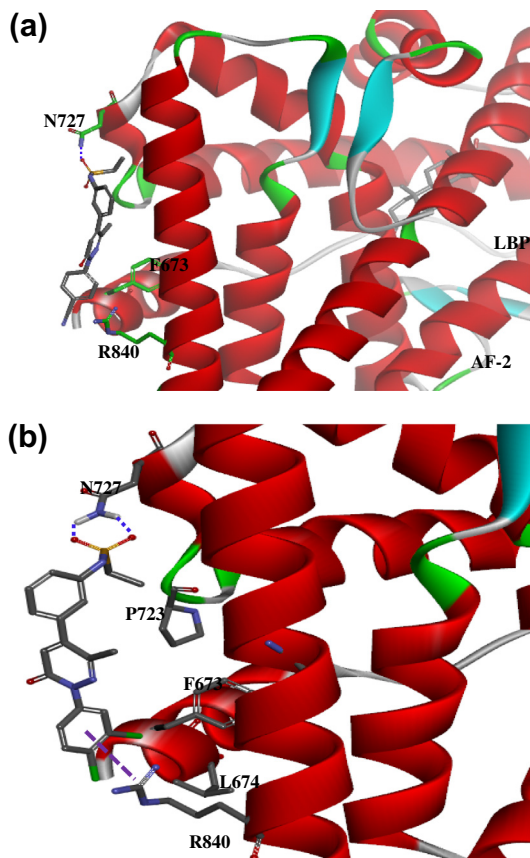


Figure 2. The binding mode for the primary hit (a) and a compound 2 (b). The blue lines represent hydrogen bond between AR residue and small molecules. The magenta line in (b) represents hydrophobic interaction between guanidinium group of R840 residue and benzene ring of compounds.

pi-stacking interaction with the guanidinium group of R840, but its surrounding residues made the shallow hydrophobic pocket consisting of F673 and L674. To evaluate our result on the binding of compound 1, we synthesized a series of compounds having hydrophobic substituents instead of 4-CN group of compound 1.

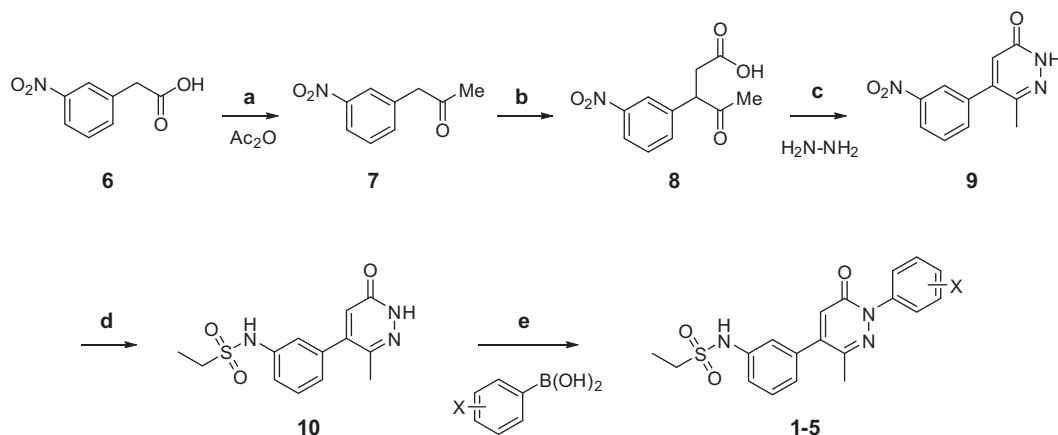
According to the Scheme 1, we synthesized desired compounds, as follows.

The synthetic route of 2-aryl-5-(2-ethanesulfonamido) pyridazine-3(2H)-one analog is depicted in Scheme 1. Commercially available 3-nitrophenylacetic acid **6** was reacted with 1-methylimidazole in acetic anhydride at room temperature to afford ketone **7**.<sup>11</sup> Alkylation of **7** with ethyl bromoacetate using lithium diisopropylamide (LDA) in THF followed by hydrolysis of ester to give acid **8**. Treatment of **8** in refluxing ethanol with hydrazine gave the cyclized dihydropyridazinones, which was oxidized with SeO<sub>2</sub> in acetic acid to provide pyridazine-3(2H)-ones **9** in good yield. Reduction of **9** with iron powder followed by sulfonylation with ethanesulfonyl chloride in pyridine to afford key intermediates **10**. Finally, desired compounds **1–5**<sup>12</sup> were obtained by coupling reaction of **10** with the appropriate aryl boronic acids or pinacol aryl boronates<sup>13</sup> using copper(II) acetate in moderate yield.<sup>14</sup>

As we expected, the substitution of hydrophobic group instead of 4-CN in the structure of compound 1 improved the inhibitory potential to LNCap cell viability and AR transcriptional activity (Table 1). Among them, compound 2 was the most active in the cell viability assay and AR luciferase assay. The binding modes of compound 1 and the most active compound 2 were shown in Fig. 2. The di-Cl group was well fitted at the position of shallow hydrophobic pocket. We further determined physicochemical properties,<sup>15,16</sup> metabolic stability<sup>17</sup> and CYP inhibition activity<sup>18</sup> of compound 2. As shown in Table 2, compound 2 showed appropriate logP

Table 1  
Viability of LNCap cells and AR luciferase activity

Compound	X	IC <sub>50</sub> (μM)	
		LNCap cell viability	AR luciferase activity
1	4-CN	39.02 ± 5.74	6.26 ± 0.35
2	3,4-di-Cl	11.57 ± 2.67	2.65 ± 0.01
3	3,5-di-Cl	22.93 ± 2.06	13.19 ± 0.03
4	3-Cl, 4-F	26.65 ± 1.62	5.07 ± 0.81
5	2-Naphthalene	18.27 ± 0.15	9.76 ± 0.27
Bicalutamide		23.79 ± 0.99	0.27 ± 0.01

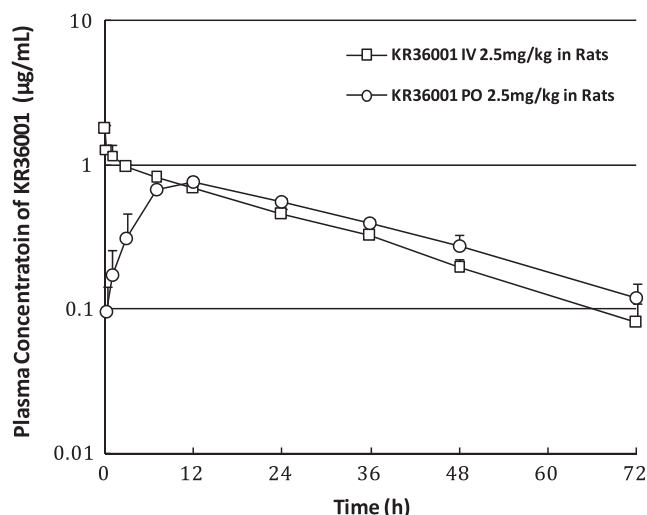


Scheme 1. Synthesis of pyridazinone analogs, reagents and conditions: (a) 1-methylimidazole, Ac<sub>2</sub>O (5 equiv), rt, 56%; (b) (i) LDA, BrCH<sub>2</sub>COOEt, THF, −78 °C to 0 °C, 5 h, 80%; (ii) 2N-NaOH, MeOH; (c) (i) H<sub>2</sub>NNH<sub>2</sub>, EtOH, reflux, 3 h, 84%; (ii) SeO<sub>2</sub>, AcOH, 100 °C, 3 h, 95%; (d) (i) Fe powder, c-HCl, EtOH, reflux, 2 h, 87%; (ii) EtSO<sub>2</sub>Cl, pyridine, 50 °C, 2 h, 74%; and (e) Aryl boronic acids or pinacol aryl boronate, Cu(OAc)<sub>2</sub>, Et<sub>3</sub>N, 4 Å molecular sieves, CH<sub>2</sub>Cl<sub>2</sub>, rt, 40–85%.

**Table 2**

Physicochemical properties, metabolic stability, CYP inhibition of thiazole derivatives

Compound	Physicochemical properties		CYP <sup>a</sup>		MS
	Log <i>P</i>	PAMPA permeability	3A4 (%)	2D6 (%)	Rat, in vitro
<b>2</b>	3.82 ± 0.03	−5.86 ± 0.06	6.7	0	>99%

<sup>a</sup> Inhibition at 10 μM CYP concentration (%).**Figure 3.** Plasma concentration-time plots after an intravenous (□) and oral (○) administration of compound **2** in SD male rats (*n* = 3).

values and medium permeability against artificial permeable membrane. In the metabolic stability assay, compound **2** remained 99% after 1 h incubation with rat liver microsomes. Compound **2** did not show the strong CYP inhibition activity. In in vitro assay, compound **2** exhibited an acceptable in the permeability, metabolic stability and CYP inhibition, but good in vitro activity may not reflect good in vivo efficacy. Therefore, we further investigated the in vivo pharmacokinetic profile of compound **2**. As shown in Figure 3 and Table 3, after oral administration of a 2.5 mg/kg dose of compound **2** to rats, the peak plasma concentration (*C*<sub>max</sub>) of 0.767 μg/mL was observed at 10.3 h. The elimination half-life for compound **2** following oral administration was 21.6 h in rats. Compound **2** showed perfect oral bioavailability (*F* = 102%) and low blood clearance (*CL* = 84.4 mL/kg/h) in rats.

In this study, we synthesized the BF-3 binding small molecules without affecting natural ligand binding, a series of pyridazinone-based compounds, to inhibit the viability of AR-dependent human prostate LNCap cells and AR activity combining with the computational method, having a good physicochemical and PK property.

**Table 3**Pharmacokinetic parameters after an intravenous and oral administration of compound **2** in SD male rats (*n* = 3)

Parameters	I.v. (2.5 mg/kg)	P.o. (2.5 mg/kg)
<i>T</i> <sub>max</sub> (h)	–	10.3 ± 2.9
<i>C</i> <sub>max</sub> (μg/mL)	–	0.767 ± 0.055
<i>T</i> <sub>1/2</sub> (h)	19.2 ± 4.5	21.6 ± 2.9
AUC <sub>0–72 h</sub> (μg h/mL)	27.5 ± 2.4	26.8 ± 3.4
AUC <sub>0–∞</sub> (μg h/mL)	29.8 ± 3.0	30.5 ± 4.9
<i>CL</i> (mL/kg/h)	84.4 ± 7.9	–
<i>V</i> <sub>ss</sub> (mL/kg)	2250 ± 259	–
<i>MRT</i> (h)	26.9 ± 4.2	34.9 ± 6.3
<i>F</i> (%)	–	102.5 ± 16.4

Furthermore, we want to seriously optimize for our compound **2** to discovery a new prostate cancer treatment.

## References and notes

- Brinkmann, A. O.; Blok, L. J.; de Ruiter, P. E.; Doesburg, P.; Steketee, K.; Berrevoets, C. A.; Trapman, J. J. *Steroid Biochem. Mol. Biol.* **1999**, *69*, 307.
- Quigley, C. A.; De Bellis, A.; Marschke, K. B.; El-Awady, M. K.; Wilson, E. M.; French, F. S. *Endocr. Rev.* **1995**, *16*, 271.
- Greenlee, R. T.; Taylor, M.; Bolden, S.; Wingo, P. A. *CA Cancer J. Clin.* **2000**, *50*, 7.
- Estebanez-Perpiña, E.; Moore, J. M.; Mar, E.; Delgado-Rodriguez, E.; Nguyen, P.; Baxter, J. D.; Buehrer, B. M.; Webb, P.; Fletterick, R. J.; Guy, R. K. *J. Biol. Chem.* **2005**, *280*, 8060.
- Buzon, V.; Carbó, L. R.; Estruch, S. B.; Fletterick, R. J.; Estebanez-Perpiña, E. *Mol. Cell. Endocrinol.* **2012**, *348*, 394.
- Ryan, C. J.; Tindall, D. J. *J. Clin. Oncol.* **2011**, *29*, 3651.
- Estebanez-Perpiña, E.; Arnold, A. A.; Nguyen, P.; Rodrigues, E. D.; Mar, E.; Bateman, R.; Pallai, P.; Shokat, K. M.; Baxter, J. D.; Guy, R. K.; Webb, P.; Fletterick, R. J. *Proc. Natl. Acad. Sci. USA* **2007**, *104*, 16074.
- Lack, N. A.; Axerio-Cilies, P.; Tavassoli, P.; Han, F. Q.; Chan, K. H.; Feau, C.; LeBlanc, E.; Guns, E. T.; Guy, R. K.; Rennie, P. S.; Cherkasov, A. *J. Med. Chem.* **2011**, *54*, 8563.
- (a) *Cell culture*: Human prostate cancer LNCap cells were cultured in RPMI1640 (Hyclone, UT) supplemented with 10% fetal bovine serum (FBS, Hyclone), 100 U/ml of penicillin and 100 μg/ml of streptomycin in humidified atmosphere of 5% CO<sub>2</sub> at 37 °C. The culture medium was changed every 3 days. (b) *Cell viability assay*: Cells were seeded in a 96-well plate at 4 × 10<sup>3</sup> cells/well, cultured for 24 h and then incubated with compounds for 2 days. Then, cell viability was measured in triplicates by the Cell Counting Kit-8 (Dojindo Molecular Technologies, ML) according to the manufacturer's protocol. Absorbance was measured by using Wallac EnVision microplate reader (PerkinElmer, Finland). (c) *AR reporter luciferase assay*: LNCap cells were seeded in a 12-well plate at 8 × 10<sup>4</sup> cells/well. After 24 h, cells were transduced by SureENTRY transduction reagent with Cignal Lenti AR reporter (5 × 10<sup>5</sup> TU; SABioscience, MD) in RPMI1640 with 10% FBS according to the manufacturer's protocol. After 2 days, medium was changed to RPMI1640 with 10% FBS, 1% antibiotics and 1% NEAA, and then transduced cells were selected in culture medium with 30 μg/ml of puromycin (Sigma, MO). After puromycin selection, selected cells (1.5 × 10<sup>4</sup> cells/well) were incubated in a 96-well plate for 1 day and treated with compounds for 1 day. Then, AR activation was evaluated by luciferase reporter assay (Promega, WI).
- Wu, G.; Robertson, D. H.; Brooks, C. L., III; Vieth, M. J. *Comput. Chem.* **2003**, *24*, 1549.
- Tran, K. V.; Bickar, D. J. *Org. Chem.* **2006**, *71*, 6640.
- General experimental methods and analytical data for the compounds*: <sup>1</sup>H NMR spectra were recorded on a Bruker Fourier AG-300 spectrometer. Chemical shifts are expressed as δ values in parts per million (ppm), relative to TMS. Coupling constant (*J*) was reported in Hertz unit (Hz). High-resolution mass spectra (HRMS) was measured on a JMS-700 mass spectrometer (JEOL, Japan) using electron impact (EI) method. *N*-(3-(1-(4-cyanophenyl)-3-methyl-6-oxo-1,6-dihydropyridazin-4-yl)phenyl)ethanesulfonamide (**1**): <sup>1</sup>H NMR (300 MHz, CDCl<sub>3</sub>) δ 7.95 (d, *J* = 8.4 Hz, 2H), 7.79 (d, *J* = 8.4 Hz, 2H), 7.46 (dd, *J* = 7.7, 7.6 Hz, 1H), 7.31 (d, *J* = 7.7 Hz, 1H), 7.30 (s, 1H), 7.14 (d, *J* = 7.6 Hz, 1H), 6.92 (s, 1H), 3.20 (q, 2H), 2.32 (s, 3H), 1.41 (t, 3H). HRMS (EI, M<sup>+</sup>): calcd for C<sub>20</sub>H<sub>18</sub>N<sub>4</sub>O<sub>3</sub>S: 394.1100, found: 394.1102; *N*-(3-(1-(3,4-dichlorophenyl)-3-methyl-6-oxo-1,6-dihydropyridazin-4-yl)phenyl)ethanesulfonamide (**2**): <sup>1</sup>H NMR (300 MHz, CDCl<sub>3</sub>) δ 7.88 (d, *J* = 2.3 Hz, 1H), 7.76 (br s, NH), 7.65 (dd, *J* = 8.7, 2.3 Hz, 1H), 7.55 (d, *J* = 8.7 Hz, 1H), 7.45 (dd, *J* = 7.7, 7.6 Hz, 1H), 7.32 (d, *J* = 7.7 Hz, 1H), 7.30 (s, 1H), 7.13 (d, *J* = 7.6 Hz, 1H), 6.93 (s, 1H), 3.19 (q, 2H), 2.30 (s, 3H), 1.39 (t, 3H). HRMS (EI, M<sup>+</sup>): calcd for C<sub>19</sub>H<sub>17</sub>Cl<sub>2</sub>N<sub>3</sub>O<sub>3</sub>S: 437.0368, found: 437.0364; *N*-(3-(1-(3,5-dichlorophenyl)-3-methyl-6-oxo-1,6-dihydropyridazin-4-yl)phenyl)ethanesulfonamide (**3**): <sup>1</sup>H NMR (300 MHz, CDCl<sub>3</sub>) δ 7.63 (s, 2H), 7.41 (dd, *J* = 7.7, 7.6 Hz, 1H), 7.31 (s, 1H), 7.22 (d, *J* = 7.7 Hz, 1H), 7.19 (s, 1H), 7.09 (d, *J* = 7.6 Hz, 1H), 6.83 (s, 1H), 6.64 (br s, NH), 3.14 (q, 2H), 2.24 (s, 3H), 1.35 (t, 3H). HRMS (EI, M<sup>+</sup>): calcd for C<sub>19</sub>H<sub>17</sub>Cl<sub>2</sub>N<sub>3</sub>O<sub>3</sub>S: 437.0368, found: 437.0364; *N*-(3-(1-(3-chloro-4-fluorophenyl)-3-methyl-6-oxo-1,6-dihydropyridazin-4-yl)phenyl)ethanesulfonamide (**4**): <sup>1</sup>H NMR (300 MHz, CDCl<sub>3</sub>) δ 7.81 (dd, *J* = 7.6, 2.2 Hz, 1H), 7.63 (m, 2H), 7.47 (dd, *J* = 7.7, 7.6 Hz, 1H), 7.28 (d, *J* = 7.7 Hz, 1H), 7.27 (s, 1H), 7.15 (d, *J* = 7.6 Hz, 1H), 6.89 (s, 1H), 6.69 (br s, NH), 3.20 (q, 2H), 2.30 (s, 3H), 1.41 (t, 3H). HRMS (EI, M<sup>+</sup>): calcd for C<sub>19</sub>H<sub>17</sub>ClF<sub>2</sub>N<sub>3</sub>O<sub>3</sub>S: 421.0663, found: 421.0662; *N*-(3-(3-methyl-1-(naphthalen-2-yl)-6-oxo-1,6-dihydropyridazin-4-yl)phenyl)ethanesulfonamide (**5**): <sup>1</sup>H NMR (300 MHz, CDCl<sub>3</sub>) δ 8.17 (d, *J* = 2.1 Hz, 1H), 7.95 (d, *J* = 8.7 Hz, 1H), 7.89 (m, 2H), 7.76 (dd, *J* = 2.1, 8.7 Hz, 1H), 7.52 (m, 2H), 7.45 (dd, *J* = 7.7, 7.6 Hz, 1H), 7.20 (br s, NH), 7.29 (m, 2H), 7.16 (d, *J* = 7.6 Hz, 1H), 6.96 (s, 1H), 3.18 (q, *J* = 7.4, 14.8 Hz, 2H), 2.33 (s, 3H), 1.40 (t, *J* = 7.4 Hz, 3H). HRMS (EI, M<sup>+</sup>): calcd for C<sub>23</sub>H<sub>21</sub>N<sub>3</sub>O<sub>3</sub>S: 419.1304, found: 419.1307.
- (a) Ishiyama, T.; Murata, M.; Miyaura, N. *J. Org. Chem.* **1995**, *60*, 7508; (b) Gerbino, D. C.; Mandolesi, S. D.; Schmalz, H. G.; Podesta, J. C. *Eur. J. Org. Chem.* **2009**, 3964.
- (a) Patent WO2008/16239; (b) Asano, T.; Yamazaki, H.; Kasahara, C.; Kubota, H.; Kontani, T.; Harayama, Y.; Ohno, K.; Mizuhara, H.; Yokomoto, M.; Misumi, K.; Kinoshita, T.; Ohta, M.; Tkeuchi, M. *J. Med. Chem.* **2012**, *55*, 7772.

15. *Log P*: *Log P* is measured by a pH-metric method, based on a two-phase acid–base titration in a mixture of water and octanol using GLpKa system by Sirius.
16. *Parallel artificial membrane permeability (PAMPA) permeability*: Donor solution (500  $\mu$ M) was prepared by diluting 1 mM DMSO compound stock solution using the diluted system buffer (pH adjusted to 7.4). Five microliters lipid solution was applied to each filter membrane. Donor solution (150  $\mu$ L) was added to each well of the filter plate. The filter plate was then put onto a receiver plate with preloaded acceptor sink buffer. The sandwich was incubated at room temperature for 16 h. Samples were taken from both receiver and donor sides at the end of the incubation and analyzed using UV spectrometer. Donor solutions were also analyzed for initial concentration.
17. *Metabolic stability*: Using rat liver microsomes, the amount of parent compound remaining after 1 h incubation. The concentration of the used compound is 5 mM and protein concentration is 1 mg/mL.
18. *CYP3A4 enzyme assay*: The assay was carried out using fluorometric enzyme assays with Vivid CYP3A4 assay kit (PanVera, USA, CA) in a 96-well microtiter

plate following the manufacturer's instruction with some modification. The compounds including ketoconazole known as CYP3A4 inhibitor were prepared in acetonitrile to give final concentrations of 10 mM. NADP generating solution (1.0 mM NADPb, 3.3 mM glucose-6-phosphate, 3.3 mM  $\text{MgCl}_2 \cdot 6\text{H}_2\text{O}$ , and 0.4 U/mL glucose-6-phosphate dehydrogenase in 10 mM  $\text{KPO}_4$ , pH 8.0) was added to each well of the microtiter plate followed by the vehicle acetonitrile (control) and the test samples. The plate was covered and then incubated at 37 °C for 20 min. Enzyme reaction was initiated by the addition of enzyme/substrate (E/S) mixture (0.5 pmol recombinant human CYP3A4 enzyme and 5 mM dibenzylfluorescein, DBF). The plate was further incubated for 20 min, followed by the addition of the stop solution to terminate the enzyme activity. Background reading was measured in a similar manner except for the E/S mixture which was added after the enzyme reaction was terminated. The fluorescence of DBF metabolite fluorescein was measured on a fluorescence plate reader with an excitation wavelength of 485 nm and an emission wavelength of 530 nm.